

# Hydrothermal Synthesis of Blue-Fluorescent Monolayer BN and BCNO Quantum Dots for Bio-imaging Probes

Qi Xue<sup>†</sup>, Huijie Zhang<sup>‡</sup>, Minshen Zhu<sup>†</sup>, Zifeng Wang<sup>†</sup>, Zengxia Pei<sup>†</sup>, Yang Huang<sup>†</sup>, Yan Huang<sup>†</sup>, Xiufeng Song<sup>#</sup>, Haibo Zeng<sup>#</sup>, and Chunyi ZHI<sup>†§\*</sup>

<sup>†</sup> Department of Physics and Materials Science, City University of Hong Kong, Hong Kong, China.

<sup>‡</sup> The Key Laboratory of Carbohydrate Chemistry and Biotechnology, Ministry of Education, School of Biotechnology, Jiangnan University, Wuxi, Jiangsu, China.

<sup>#</sup> Institute of Optoelectronics and Nanomaterials (ION) and Herbert Gleiter Institute of Nanoscience (HGI), College of Materials Science and Engineering, Nanjing University of Science and Technology, Nanjing, China.

<sup>§</sup> Shenzhen Research Institute, City University of Hong Kong, Shenzhen, China

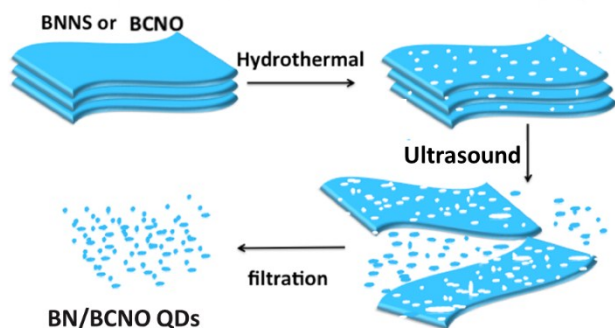


Fig. S1 Preparation method of BN/BCNO QDs.

## Calculation of Quantum Yield

Quantum Yield (QY) of BN/BCNO quantum dots were calculated by comparative method using coumarin 120 in methanol as the reference. The quantum yield of BN/BCNO QDs (in water) was calculated according to

$$\Phi_s = \Phi_r \times \frac{I_s}{I_r} \times \frac{\eta_s^2}{\eta_r^2} \times \frac{A_r}{A_s}$$

Where  $\Phi$  is the quantum yield,  $I$  is measured integrated emission intensity,  $\eta$  is refractive index of the solvent and  $A$  is absorption of the reference ( $r$ ) and as-prepared QDs sample ( $s$ ).

**Table S1.** Quantum yield of BN/BCNO QDs solution (in H<sub>2</sub>O) using coumarin 120 as a reference.

sample	Absorption at 290 nm	Integrated Emission	Refractive Index	Quantum yield
Coumarin 120	0.0015	6260	1.3284	73%
BN QDs	0.0168	1739	1.3330	1.8%
BCNO QDs	0.0082	2326	1.3330	5%

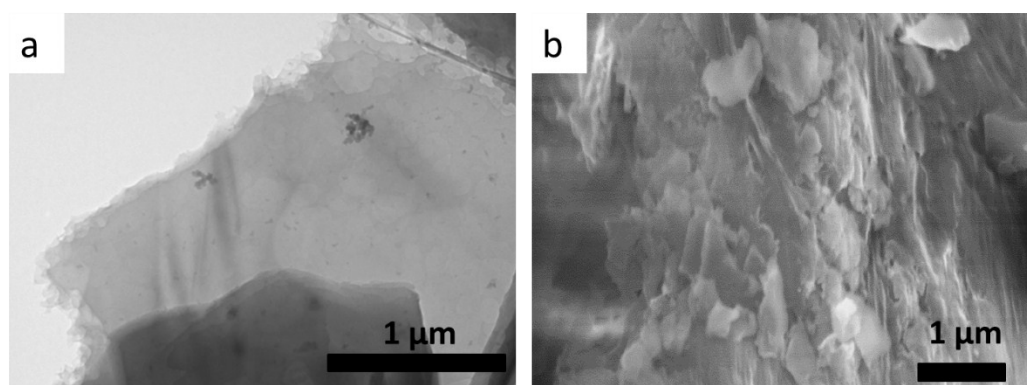


Fig.S2 TEM image of BN nanosheets (a) and SEM image of raw BCNO flakes (b).

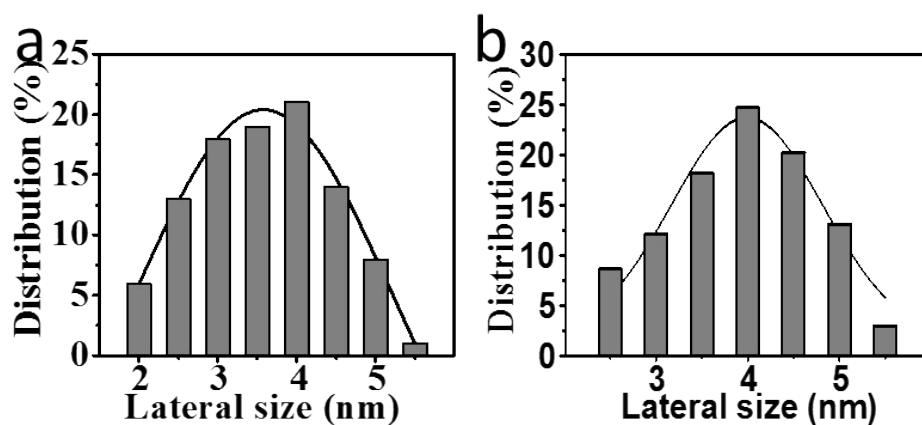


Fig.S3 Lateral size distribution of BN QDs (a) and BCNO QDs (b).

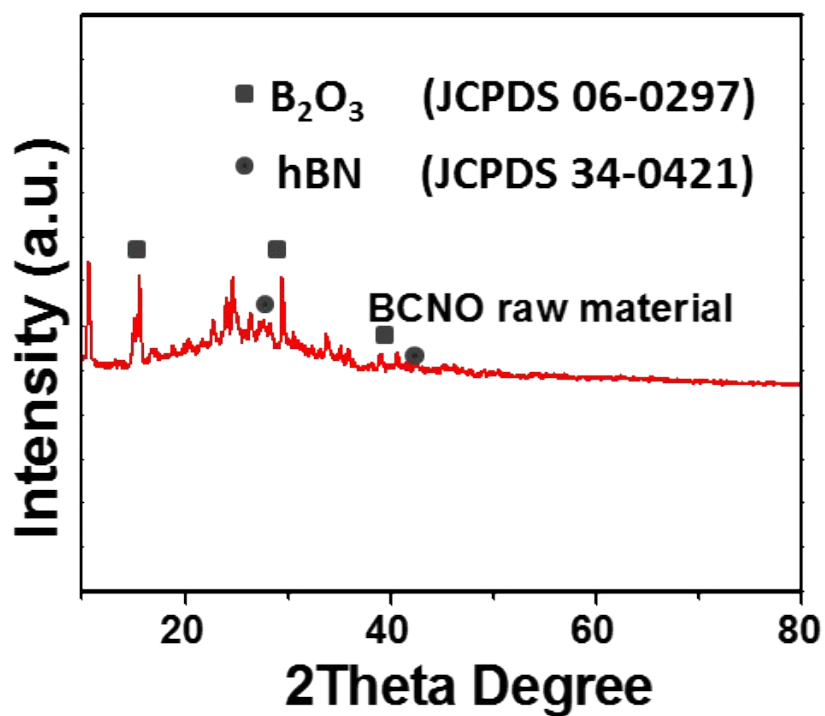


Fig. S4 XRD spectra of BCNO raw material.

The XRD spectra of BCNO raw material was exhibited in Fig. S4. Two distinct peaks marked with block corresponding to crystalline B<sub>2</sub>O<sub>3</sub>. Moreover, there were two hBN peaks indicating the formation of BN. The XRD spectra was similar to reported works.<sup>1</sup>

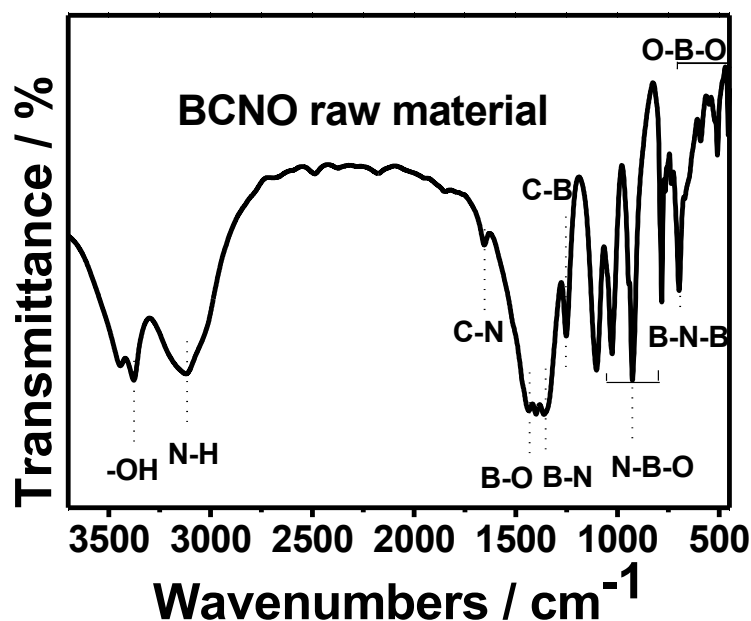


Fig. S5 FT-IR spectra of BCNO raw material.

Two bands at around 1400 and 800 cm<sup>-1</sup> correspond to characteristic bands of B-N vibrations in h-BN. C-B bond appeared at around 1200 cm<sup>-1</sup>, indicating that doped C leads to BCNO nanostructure. The vibrations at around 1650 cm<sup>-1</sup> suggests suggests the formation of the C-N bonds<sup>2,3</sup>

The chemical compositions and structure of BCNO raw material were analyzed by X-ray photoelectron spectroscopy (XPS). Fig. S5a shows the BCNO raw material was composed of B, C, N and O elements. In Fig. S5b, strong peak at 284.6 was ascribed to be C-C, C=C or contamination on the tape which is a tool in the XPS tests. C-B, C-N, C-N/C-O-B bonds were centered at 283.6 eV, 286, 287.3 respectively.<sup>3</sup> In Fig. S5c, the B1s signal could be well divided into three peaks, including B-O, B-N and B-C. Since the B-C is the main peak, which indicate the BCNO composed of large fraction of B-C phase. For N1s signal, the main peak is pyridinic N, the rest weak peaks

corresponds to C-B-N and graphitic N bondings.<sup>3,5</sup>

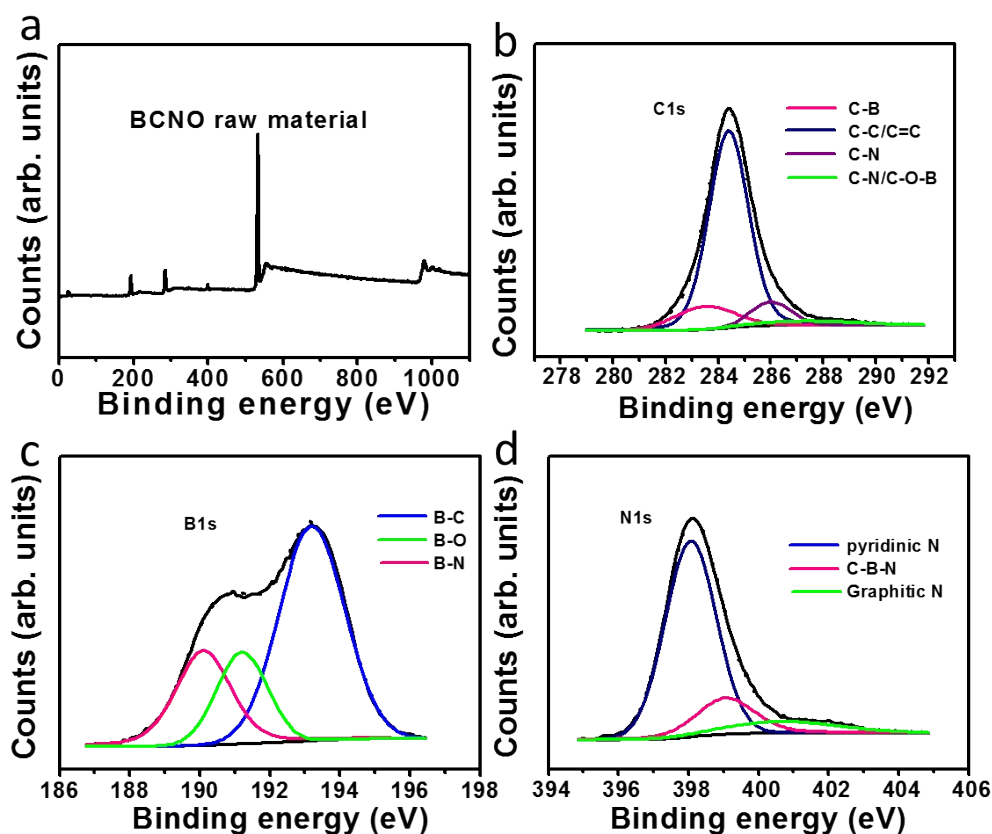


Fig. S6 (a) XPS fully scanned spectrum of BCNO raw material. (b, c, d) and d are high resolution XPS spectra of B1s, C1s and N1s of BCNO raw material.

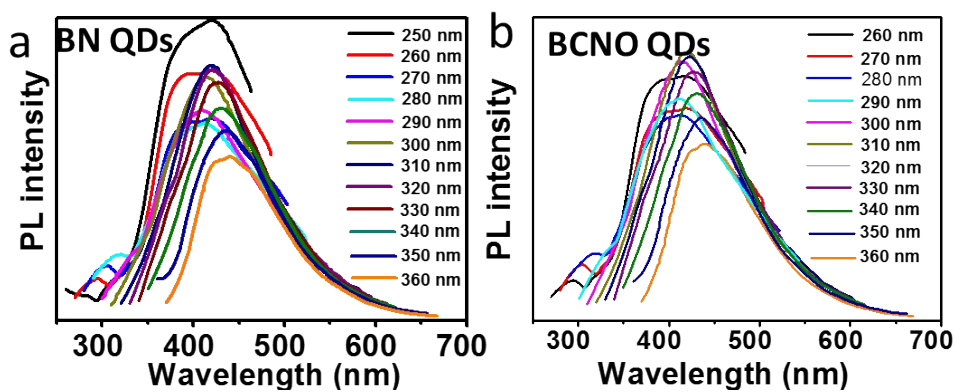


Fig. S7 (a) and (b) are the photoluminescence spectra of BN and BCNO QDs.

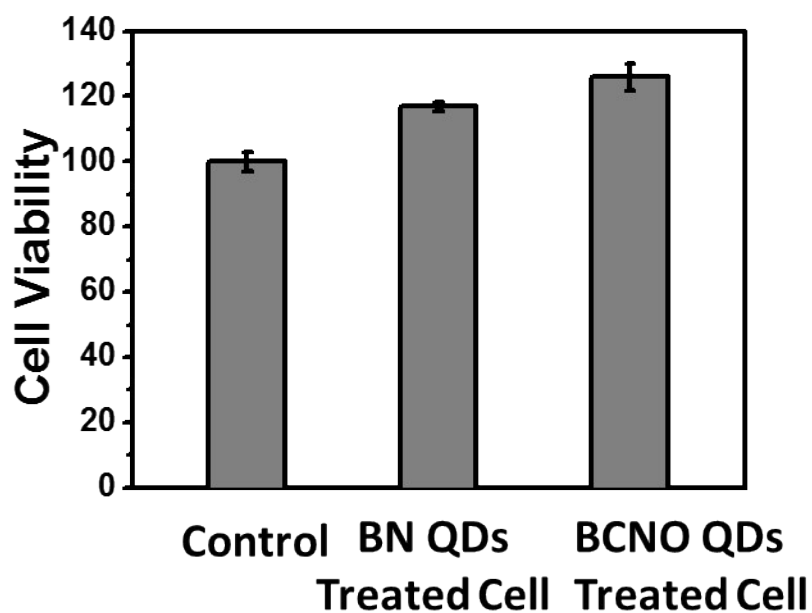


Fig.S8 Cell viability of RAW264.7 cells at 37 °C under different BN and BCNO QDs (15ug/ mL).

#### References:

- (1). (a)B.W. Nuryadin, T.P. Pratiwi, F. Iskandar, M. Abdullah, K. Khairurrijal, T. Ogi, K. Okuyama, *Advanced Powder Technology* 2014, 25, 891.(b)X. Zhang, Z. Lu, J. Lin, Y. Fan, L. Li, X. Xu, L. Ho, F. Meng, J. Zhao, C. Tang, *ECS Journal of Solid State Science and Technology*,2013, 2, R39.
- (2). Li, X. L.; Hao, X. P.; Zhao, M. W.; Wu, Y. Z.; Yang, J. X.; Tian, Y. P.; Qian, G. D. *Advanced Materials* 2013, 25, 2200.
- (3). (a)Lu, F.; Zhang, X. H.; Lu, Z. M.; Xu, X. W.; Tang, C. C. *Journal of Luminescence* 2013, 143, 343(b) Chu, Z. Y.; Kang, Y.; Jiang, Z. H.; Li, G. Y.; Hu, T. J.; Wang, J.; Zhou, Z. F.; Li, Y.

H.; Wang, X. J. Rsc Advances 2014, 4, 26855(c) Zhang, X. H.; Jia, X. B.; Liu, H.; Lu, Z. M.; Ma, X. K.; Meng, F. B.; Zhao, J. L.; Tang, C. C. Rsc Advances 2015, 5, 40864.

- (4). (a) Mahen, E. C. S.; Nuryadin, B. W.; Iskandar, F.; Abdullah, M.; Khairurrijal In Padjadjaran International Physics Symposium 2013; Joni, I. M., Panatarani, C., Eds., 2013; Vol. 1554(b) Liu, X.; Qiao, Y.; Dong, G.; Ye, S.; Zhu, B.; Zhuang, Y.; Qiu, J. Journal of The Electrochemical Society 2009, 156, P81.
- (5). Mannan, M. A.; Noguchi, H.; Kida, T.; Nagano, M.; Hirao, N.; Baba, Y. Thin Solid Films 2010, 518, 4163.